Journal of Water Resource and Protection, 2020, 12, 657-671
https://www.scirp.org/journal/jwarp
ISSN Online: 1945-3108
ISSN Print: 1945-3094

Assessment of Vulnerability to Groundwater Pollution in the Lobo Watershed at Nibéhibé (Central-West, Côte d'Ivoire)

Yiwa Monique Kamenan[1*], Oi Mangoua Jules Mangoua[1,2*], Brou Dibi[1], Sampah Eblin Georges[1], Kouakou Lazare Kouassi[1], Kouamé Auguste Kouassi[2]

[1]Laboratory of Science and Technology of Environment, Jean Lorougnon Guédé University, Daloa, Côte d'Ivoire
[2]Laboratory Geosciences et Environment, Nangui Abrogoua University, Abidjan, Côte d'Ivoire
Email: *mjul_2@yahoo.fr, *mkamenan@gmail.com, dibrou2003@yahoo.fr, sageblin@gmail.com, k_lazare@yahoo.fr, kouameauguste@yahoo.fr

How to cite this paper: Kamenan, Y.M., Mangoua, O.M.J., Dibi, B., Georges, S.E., Kouassi, K.L. and Kouassi, K.A. (2020) Assessment of Vulnerability to Groundwater Pollution in the Lobo Watershed at Nibéhibé (Central-West, Côte d'Ivoire). *Journal of Water Resource and Protection*, **12**, 657-671.
https://doi.org/10.4236/jwarp.2020.128040

Received: July 2, 2020
Accepted: August 11, 2020
Published: August 14, 2020

Abstract

Drinking water supply to people in rural areas is increasingly oriented towards the search for groundwater. However, these resources, which were once of good quality, are currently threatened by various sources of pollution points and diffuse. The objective of this study is to map the intrinsic vulnerability to groundwater pollution of the Lobo watershed in Nibéhibé. The intrinsic vulnerability mapping method, PaPRIKa adapted or PaPRI which acronym is the protection of aquifers (Pa) based on three criteria: *P* for protection, *R* for rock type, *I* represents infiltration was used. The results show three (3) vulnerability classes, which are moderate, high and very high. This map shows that the high vulnerability class (89%) dominates the study area. This predominance shows that the groundwater of the Lobo watershed is at high risk of pollution.

Keywords

Pollution, Groundwater, Vulnerability, PaPRI, Côte d'Ivoire

1. Introduction

Groundwater is of paramount importance in most parts of the world. However, this resource, which was one of good qualities, is now under threat from various sources of pollution points and diffuses contamination [1]. According to World Health Organization, approximately 1.1 billion people do not have access to safe drinking water and 2.4 billion do not have access to adequate sanitation [2]. In addition, water has now become a global strategic issue which management must be integrated in a sustainable development perspective [3]. In Côte d'Ivoire, considering the low flow rates of boreholes in the basement zone [4] [5], surface waters constitute the abundant and sustainable resource. They are exploited to meet the drinking water needs of populations in large urban centers such as Daloa. Or, the water of the Lobo River, which is treated to supply the population of Daloa township in water, is very rich in organic matter, micro-pollutants and other toxic substances that are poorly controlled, giving it unpleasant organoleptic and physical aspects [6]. Face with this unpleasant situation, the population of Daloa township has turned to groundwater for their drinking water supply. However, these waters are facing a phenomenon of anthropogenic pollution, which degrades their quality. Prevention against these pollutants is essential for their better management in a sustainable way. Methods of vulnerability to pollution due to their performance in the delimitation of protective perimeters are the most appropriate methods [7] [8]. The objective of this study is to map the intrinsic vulnerability to groundwater pollution of the Lobo watershed in Nibéhibé.

2. Material and Methods

2.1. Study Area

The Lobo river watershed located in the central western part of Côte d'Ivoire between longitudes 6˚20 and 7˚55 West and latitudes 6˚ and 6˚55 North has three main departments (Daloa, Zoukougbeu, and Vavoua) with Daloa as the regional capital (**Figure 1**). The basin's population is estimated at 1,103,059 habitants [9], with a density of 165.67 habitants per km^2. Its surface area is about

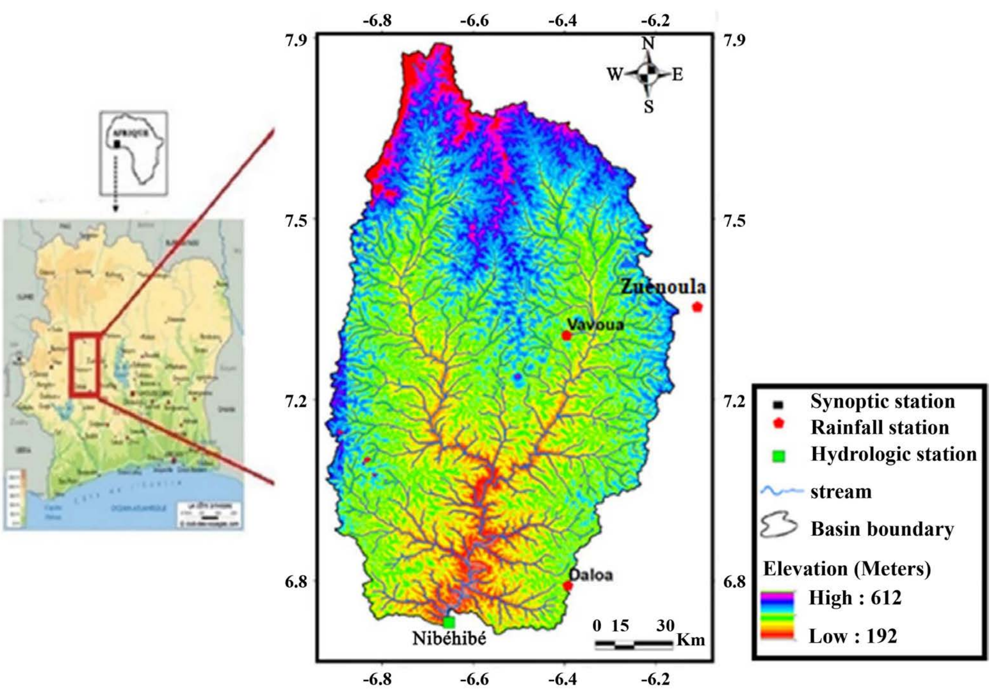

Figure 1. Study area.

7280 km^2. Drinking water supply for towns and large villages is provided by the water supply systems of the Water Distribution Company of Côte d'Ivoire (SODECI) and for the other localities by the village water system. The basin's climate is of a transitional equatorial type characterized by a rainy season from March to October and a dry season from November to February with little temperature variation [10]. The geological formations of the basin are dominated by three geological entities, namely granite that occupies almost the entire basin, shale and flysch, which are found in some places [11] and [12].

These geological formations are covered essentially by ferralitic soils moderately desaturated made of sand and clay. In terms of hydrogeology, the study area has water reserves developing in aquifers, which importance depends on the level of alteration and fracturing of the bedrock. There are therefore two types of aquifers, the alterite and fissure aquifers.

2.2. Data Collection

We used several types of data:

- 53 drilling data sheets dating from 2001 were provided by the Territorial and Hydraulic office of Daloa, from which we extracted the nature and thickness of the alterations.
- The cartographic data used are images DTM (Digital Terrain Model). They enabled to draw up the map of the slopes. The hydrographic network map allowed highlighting the drainage density map. All these combined data allowed to draw up the infiltration map of the study area.

2.3. Mapping of Vulnerability to Groundwaters Pollution in the Lobo Watershed

PaPRI method [13] is an adaptation of the PaPRIKa method with the parameters protection (*P*), the characteristics of reservoir rock (*R*) and infiltration (*I*). The lack of epikarst leads to the limitation of the number of parameters to three (3) against four (4) for PaPRIKa. The protection of aquifers based on the Protection criteria, Rock, Infiltration and Karstification (PaPRIKa) is an advancement of the methods RISKE [14] and RISKE 2 [15]. It characterizes vulnerability to infiltration, that is, the ease with which a pollutant can reach the reservoir. The interested reader can find more details on the PaPRIKa method in [16]. In the case of absence of epikarsts, PaPRI method uses three parameters instead of four for PaPRIKa: protective parameters (*P*), the characteristics of rock reservoir (*R*) and infiltration (*I*). The selection of this method meets three requirements: the method must be affordable in terms of cost, it must be technically feasible for hydrogeologists and other water-related organizations and finally it must use available data [17].

The adaptation of the PaPRIKa method to the base area should not be a problem. Indeed, most of the vulnerability methods developed have always been adapted to the different types of geological formations, taking into account the particularities of each geological formation. The current adaptation is linked to the fact that at the level of basement aquifers, we find the same hydrogeological entities as at the level of karst [8] [13] [18]. This is the soil layer, the alteration cover, which is called epikarst at the level of karst aquifers and the fractured zone, which constitutes the feeding zone for karst.

2.4. Criteria Definition

Criterion P represents all the factors contributing to water table protection against infiltration. It characterizes the capacity of reducing the movement of pollutants and their transfer rate from the surface to the water table. It mainly depends on the nature and thickness of soil (S), but also on alterites (A) and on non-saturated area (NSA) as well as its fracturing [8] [13] [18].

Criterion R represents the geological nature of the aquifer reservoir characterized by lithology and fracture [19]. It is spatialized from geological maps, land observation, data about the lithological nature and drilling sets.

Criterion I concerns infiltration conditions. This infiltration is due to various parameters that could either accelerate or delay it according to their nature. Infiltration is conditioned by two meaningful criteria: the slope and drainage density [8] [18].

The different criteria presented here contribute to the development of the final vulnerability map by successively combining these criteria through the ArcGis software by inverse distance weighted (IDW) interpolation (**Figure 2**).

2.5. Weighting Calculation

Calculation of weights or weighting coefficients is based on Saaty's [20] method of pairs comparison (**Table 1**).

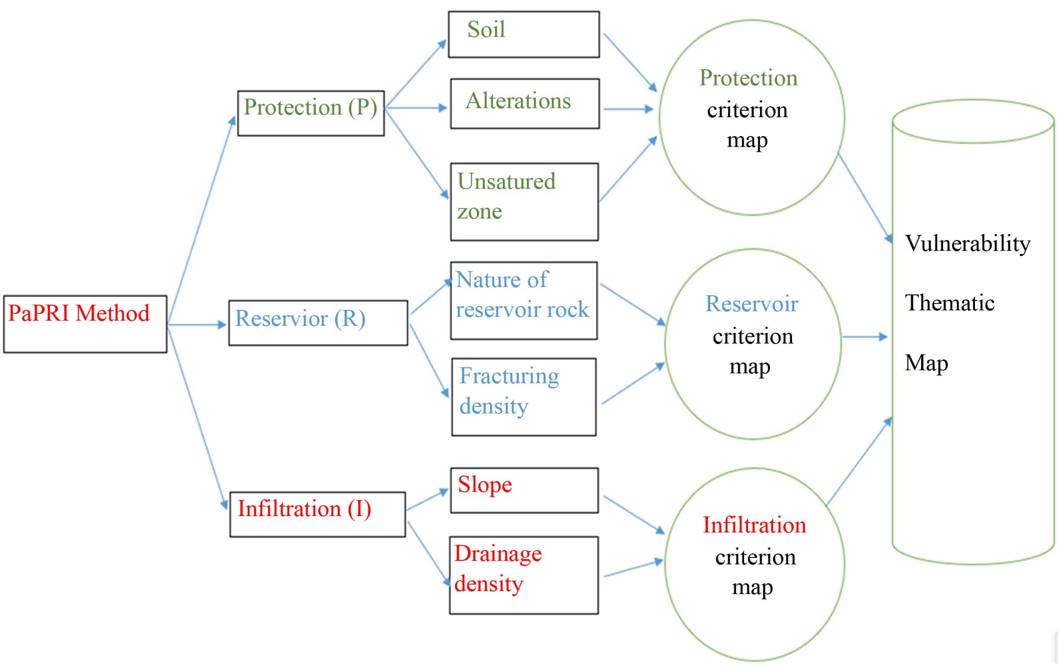

Figure 2. Conceptual model presenting the stages of the development of the vulnerability map [18].

Table 1. Verbal and numerical expression of the relative importance of a pair of factors.

Expression of a criterion compared to another	Note
Less important	1/3
Slightly less important	1/2
Same importance	1
Slightly more important	2
More important	3

The values resulting from this comparison were then integrated into an eigenvector (Equation (1)) and weighting coefficient (Equation (2) calculation for each parameter [21].

$$V_p = \sqrt[n]{\prod_{i=1}^{n} N_i} \quad (1)$$

V_{pi} = Eigen-vector of each factor; N_i = Value of each factor

$$W_i = \frac{V_{pi}}{\sum_{i=1}^{n} V_{pi}} \quad (2)$$

(W_i) = weighting coefficient of each factor.

On this basis, correlation matrices were developed for each sub-criterion to determine at the level of each grid box the value of the criterion concerned (Table 2).

2.6. Vulnerability Index Determination

The calculation of the vulnerability index is based on the DISCO method [22]:

$$V_g = iI + pP + rR \quad (3)$$

with I, P and R represent the different criteria and i, r and p the corresponding weights of the criteria. The weighting coefficients resulting from this approach are presented in Table 3.

2.7. Determination of the Vulnerability Index Colors

Five colors were used to represent the degree of index of the criteria at each point in the study area. Blue for class 0 indicating a very low index, green for class 1 indicating a low index, yellow for class 2 indicating an intermediate (moderate) index, brown for class 3 indicating a high index and red for class 4 indicating a very high index (Table 4).

2.8. Vulnerability Map Validation Method

2.8.1. Margin of Error Calculation

Vulnerability assessment is an important tool, but it is necessary to determine the quality of the information obtained from the vulnerability map. The use of geostatistical methods allows a rigorous analysis of the information and the appropriate use of the results obtained [23]. In this study, margins of error were

Table 2. Pair comparison matrix and weighting coefficient of the reservoir, infiltration and protection factors.

Protection factor (*P*)					
	NSA	Alterites	Soil	Eigen-Vector	weighting coefficient
NSA	1	1/3	2	1.49	0.32
Alterities	3	1	3	1.91	0.42
Soil	1/2	1/3	1	1.22	0.26
Roche factor (*R*)					
	Fracture	Nature of Rock	Eigen-Vector	weighting coefficient	
Fracture	1	3	2	0.63	
Nature of Rock	1/3	1	1.15	0.37	
Infiltration factor (*I*)					
	Slope	Drainage density	Eigen-Vector	weighting coefficient	
Slope	1	3	2	0.63	
Drainage density	1/3	1	1.15	0.37	

Table 3. Summary table presenting the weighting coefficient of the main factors.

Criteria	Eigen-Vector	weighting coefficient
Infiltration (*i*)	1.82	0.50
Protection (*p*)	1.22	0.20
Rock Nature (*r*) Nat	1.52	0.30

Table 4. Description of vulnerability according to coloring class index color [16].

Index values	Class	vulnerability
3.20 - 4.00	**4**	**Very high**
2.40 - 3.19	**3**	**High**
1.60 - 2.39	**2**	**Moderate**
0.80 - 1.59	**1**	**Low**
0.00 - 0.79	**0**	**Very Low**

used to verify the reliability of the vulnerability map. The calculation of the margins of error requires the determination of the uncertainties on the mean indices of the different parameters that constitute one method [7]. Uncertainty is evaluated using for this equation:

$$\Delta\overline{x} = \frac{\sigma}{\sqrt{m}} = \sqrt{\frac{1}{m(m-1)}\sum_{i=1}^{m}\left|(x_i - \overline{x})\right|^2} \tag{4}$$

with $\Delta\overline{x}$: Uncertainty on the average index of each parameter.

σ: Standard deviation of the vulnerability index of the hydrogeological parameter;

m: Number of boreholes considered;

x_i : Vulnerability index of the hydrogeological parameter to drilling *i*;

$\bar{x}$: Average vulnerability index of the hydrogeological parameter.

From the uncertainty, determined on each parameter, the margin of error itself is calculated from Equation (5).

$$E_r = \frac{\sum \Delta \bar{x}}{I_{V\_M}} \tag{5}$$

with I_{v_M}, Average Vulnerability Index for each method.

2.8.2. Validation of the Vulnerability Map by Nitrate

The validation of the pollution vulnerability map obtained by PaPRI method was tested by using nitrate concentrations. It consists of a comparison between the spatial distribution of nitrate concentrations in groundwater and the distribution of the vulnerability classes. The choice of nitrates as indicator of vulnerability is due to the fact that these ions are stable, soluble, mobile and easily reach the groundwater [24]. In this validation, the actual contaminated areas must correspond to those with the highest vulnerability index. A vulnerable area may also have a low vulnerability index because the notion of vulnerability is not synonymous with current pollution, but rather with the predisposition of these areas to possible contamination, if nothing is done to protect them.

3. Results and Discussion

3.1. Results

3.1.1. Evaluation of the Aquifer Vulnerability Factors

Thematic map of the protection factor: it shows three classes of protection index (low, moderate, and high). The study area is dominated by the moderate protection class, which occupies 97% of the study area. The remaining part of the area is evenly divided between the low and high protection classes, which respectively occupy 1.50%, and 1.50% of the study area (**Figure 3**). Moderate protection class is observed over almost the entire study area. Low and high protection zones meet respectively in the northwest and south of the basin. The margin of error on this map is 2.90%.

Thematic map of Rock or Reservoir: Analysis of the rock criteria map shows all porosity classes (low, moderate, high and very high). The Study Area is dominated by the moderate porosity class (32%) and is observed throughout the study area. The very high porosity zones occupy only (15%) of the area and are represented in bloc in the North and South. These zones are located where fracturing density is very high. The low porosity class occupies 27% of the study area and is located over almost the entire study area. This class is followed by the high porosity class, which occupies 26% of the study area (**Figure 4**). The groundwater reservoir map of the Lobo Basin has a margin of error of 3.10.

Infiltration criterion map: It is dominated by the very high infiltration class, which occupies 86% of the study area. It is found in almost the entire study area

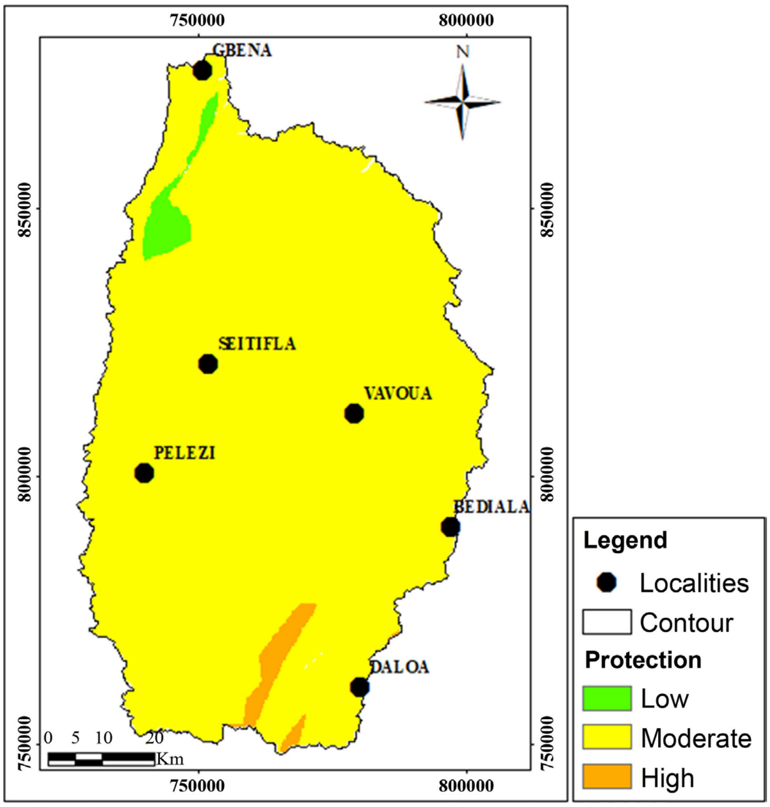

Figure 3. Protection map.

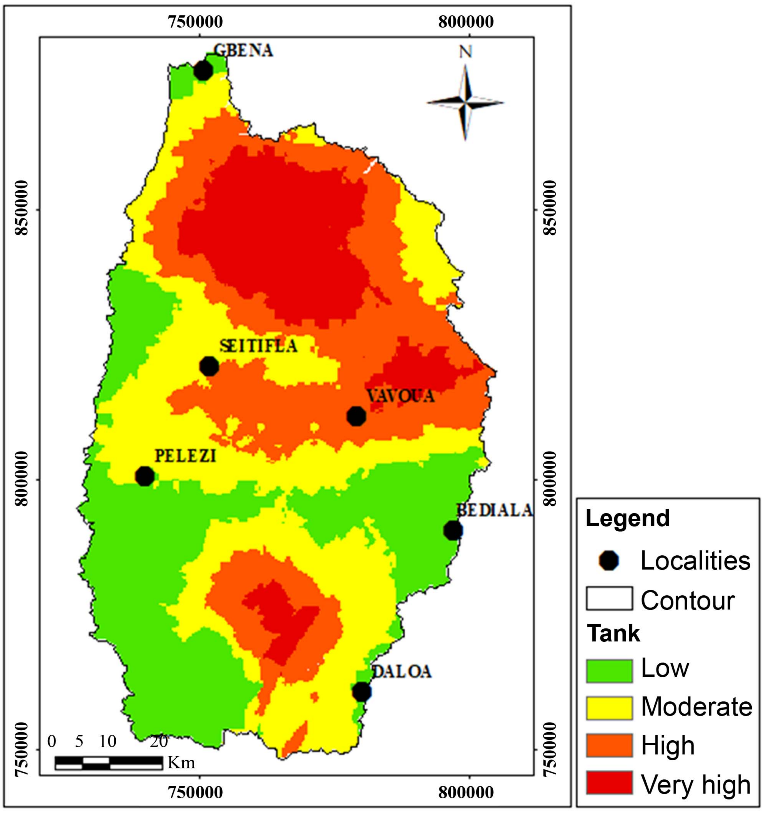

Figure 4. Reservoir map.

with high and moderate infiltration zones occupying respectively 13.80% and 0.12% of the study area (Figure 5). The margin of error on this map is 2.30%.

3.1.2. Establishing Vulnerability Map

The combination of all the criteria resulted in obtaining the pollution vulnerability map of aquifers based on the PaPRI method. The final map (Figure 6) has the particularity of highlighting the areas to be protected. The analysis of this map shows that classes with low vulnerability to pollution do not exist in the study area. Indeed, the results show that the high vulnerability class dominates the area.

Moderate, high and very high vulnerability classes respectively occupy about 9.97%, 89% and 0.98% of the total area of the study zone. These areas are considered as areas to be monitored with respect to intense anthropogenic activities that tend to pollute groundwater.

The error on the groundwater vulnerability map of the Lobo watershed in Nibéhibé is 2.50%. The overlay of the protection, reservoir and infiltration maps with different uncertainties of 0.03, 0.09 and 0.05 respectively was used to develop this map (Table 5).

3.1.3. Validation of the Vulnerability Map by Nitrate

The pollution vulnerability map was validated using nitrate (NO_3^-) contents in

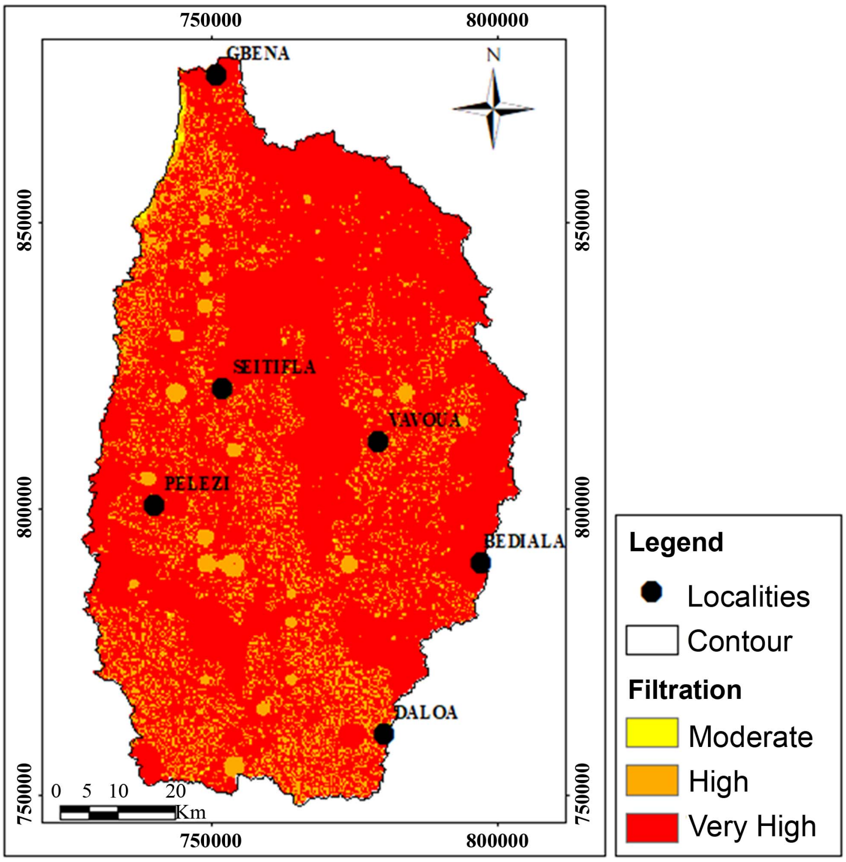

Figure 5. Infiltration map.

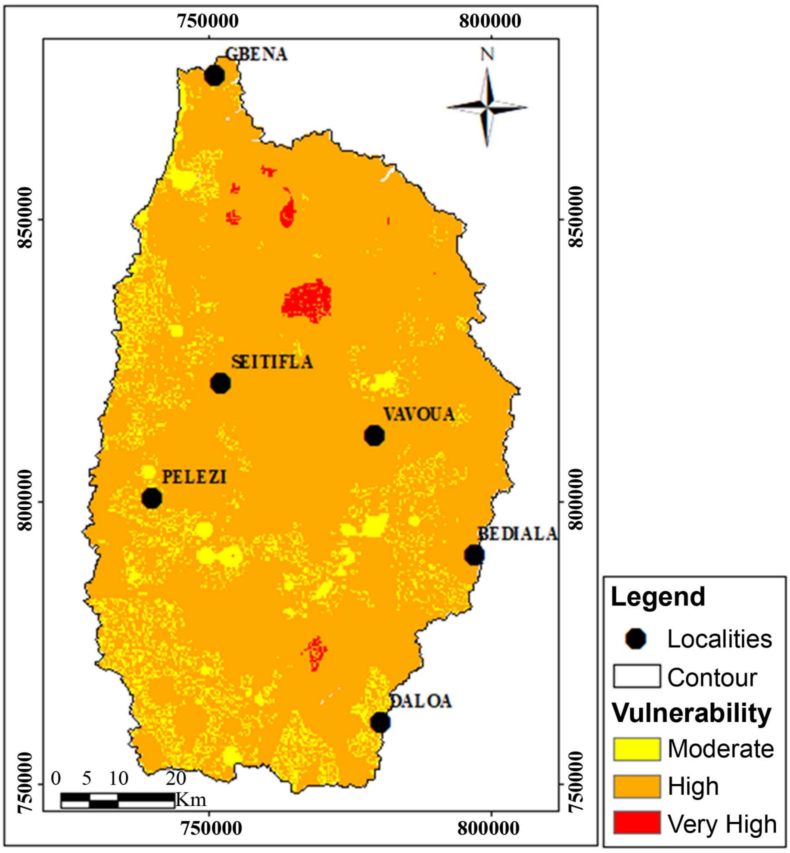

Figure 6. Pollution vulnerability map.

Table 5. Descriptive statistics of PaPRI index.

Variables	Min	Average	Max	Standard deviation	$\Delta\bar{x}$
Protection	1.13	1.51	2.54	0.42	0.03
Reservoir	1.00	1.86	3.34	0.38	0.09
Infiltration	1.40	3.51	7.6	0.20	0.05
Sum I_{v_M} = 6.88				**$\sum\Delta\bar{x} = 0.17$**	
Error E_r = 2.50%					

groundwater. The concentrations are ranged from 56.10 to 152 mg/L. These levels are above the threshold value (50 mg/L) proposed by WHO for drinking water. The spatial distribution of these levels over the entire area associated with the vulnerability map is shown on Figure 7. This map shows that all the nitrate levels coincide with the high vulnerability zone.

3.2. Discussion

Like the PaPRIKa method, the PaPRI method, specially designed for assessing intrinsic vulnerability, is based on structural factors and hydraulic behaviors in accordance with Mangin's [25] concepts developed for karsts. The factor P that characterizes the protection of the groundwater includes all the factors that can

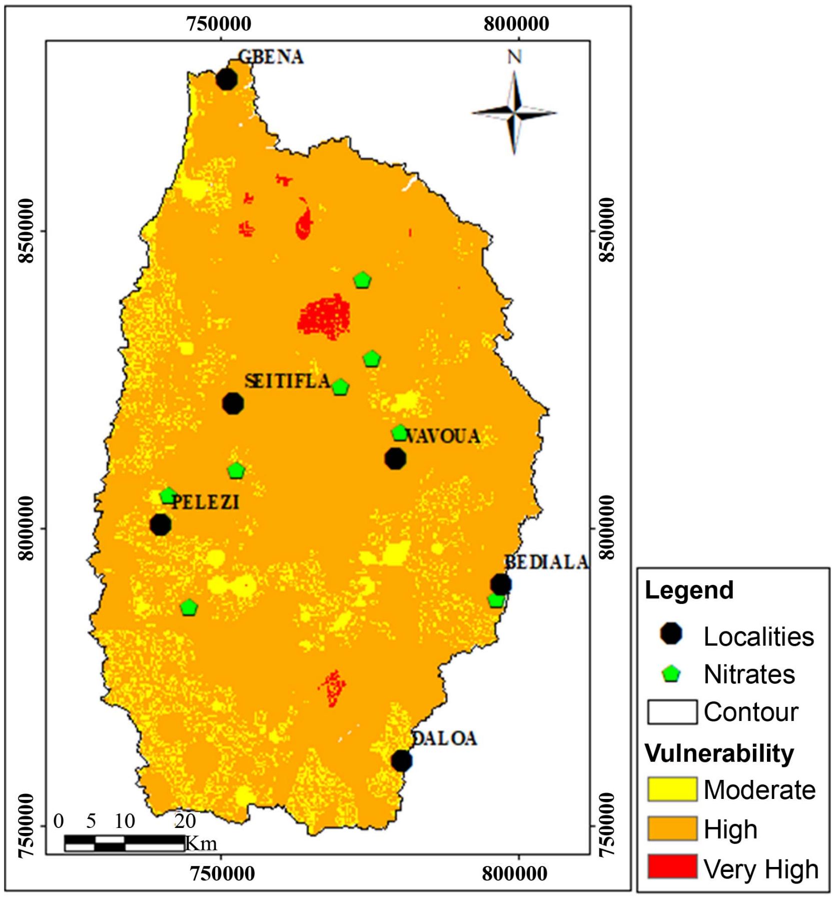

Figure 7. Final map of vulnerability to pollution validated by nitrates.

act as the first curtain that can prevent pollutants from reaching the water table. The protection criterion map of the study area is 97% dominated by the moderate protection class. Indeed, these layers with moderate thickness and nature result from the superposition of the soil layers, alterites and the NSA. They prevent the transport of pollutants, reduce the infiltration speed and therefore prevent these pollutants from reaching the groundwater. Then, the rock criterion characterized by its capacity to contain water comes from the lithology of the rocks that constitute the aquifer and its fracturing density. The analysis of the rock criterion map of the Lobo watershed is dominated by the average porosity, which covers more than 31.76% of the area. These moderate porosities can be explained by a moderate fracturing density since the reservoir rock is the result of the alteration of healthy rock (mostly granitic and some gneiss). These results are in line with those of [13], which indicate that, at level of the basement formations, the criterion *R* is highly dependent on fracturing and alteration that affect the hydrodynamic properties of the reservoir. As for the infiltration factor, it determines the capacity to delay or accelerate pollutant infiltration. This factor depends on the slope and drainage density. However, the slope remains the most important parameter. Indeed, the study area has overall 76.90% of slight slopes. This is consistent with the work of [21], when they report that in areas with slight slopes and high permeability, groundwater availability varies from good to excellent. This means that in areas with slight slopes, water stays in contact with the ground longer and facilitates its infiltration compared to areas with high slopes. Water is then quickly drained away, as indicated by the work of [26], which showed that the steeper the slopes and greater the drainage density are, the lower the probability of water infiltration towards the groundwater is and vice-versa. Finally, the vulnerability map highlights the high vulnerability class, which occupies 89% of the study area. This high vulnerability is explained by the high fracturing density, which gives the geological formations good porosity with slight slopes that would favor water infiltration from the surface to the groundwater. We add to that the average thickness of the protective layers, which more or less facilitates the vertical transport of the contaminant. These results are similar to those of [7] which underlined the importance of soil type, indicating that the presence of highly permeable soil associated with a shallow water table and high recharge would be a favorable condition to increase the vulnerability to the pollution of aquifers. The PaPRI method gave good results in this work as shown in the work of [8] [13] [18] but experienced some difficulties in developing the vulnerability maps. These difficulties essentially lie in the number of criteria to be taken into account and in the limits of the classes and ratings assigned to them [23]. Despite these various limitations, the vulnerability map remains reliable. The reliability of this map was tested on the one hand by determining the margin of error on the vulnerability map, as did [7] and on the other hand by the nitrate concentrations obtained in the study area. Indeed, many authors to validate pollution vulnerability maps have used nitrate concentrations [27] [28] [29] [30]. In the present study, the low value of the margin of error on each map reflects both the good quality of the scores assigned to the various parameters and the adaptation of these methods to the study area. Indeed, the margin of error calculated to assess the method gave 2.8%. This margin of error is lower than those obtained by [7] in M'bahiakro, as well as [24] in Agboville and is in the same range as [31] in Adiaké. Concerning the coincidence rate of nitrate concentrations in the different vulnerability classes, a coincidence rate of nitrate concentrations above 50 $mg \cdot L^{-1}$ with the high vulnerability classes is 100%. This value remains higher than those obtained by [32] in the Metline water table (northeastern Tunisia) with coincidence rates of 79% for the SI method and 80.2% obtained by [33] by the AMC method.

4. Conclusion

The vulnerability to groundwater pollution of the Lobo watershed in Nibéhibé was mapped by using the intrinsic vulnerability method PaPRI. The results of the moderate, high and very high vulnerability classes occupy approximately 9.97%, 89% and 0.98% of the total surface area of the study area, respectively. These areas are considered as areas to be monitored with respect to intense anthropogenic activities that tend to pollute groundwater. The overlay of high nitrate concentrations (>50 mg·L^{-1}) and high vulnerability zones are 100% with a margin of error of 2.80%, which shows that the intrinsic vulnerability map suited well to the study area.

Acknowledgements

This study was financed by the Institut of Research for Development (IRD) through the PReSeD 2 project entitled Elaboration of an integrated water resources management model for the improvement of the drinking water supply of the commune of Daloa.

Conflicts of Interest

The authors declare no conflicts of interest regarding the publication of this paper.

References

[1] Haoua, A., Mahaman, S.L. and Abdou, S.M. (2014) Caractérisation hydro chimique des eaux souterraines de la région de Tahoua (Niger). *Journal of Applied Biosciences*, **80**, 7161-7172. https://doi.org/10.4314/jab.v81i1.6

[2] OMS (2008) Rapport sur la sante dans le monde, Les soins de santé primaires-maintenant plus que jamais. OMS, Genève, 149 p.

[3] Servais, P., Billen, G., Garcia-Armisen, T., George, I., Goncalvez, A. and Thibert, S. (2009) La contamination microbienne dans le bassin de la Seine, Edition. Agence de l'Eau Seine Normandie, 50 p.

[4] Ahoussi, K.E. (2008) Evaluation quantitative et qualitative des ressources en eau dans le Sud de la Côte d'Ivoire. Application de l'hydrochimie et des isotopes de l'environnement à l'étude des aquifères continus et discontinus de la région d'Abidjan-Agboville. Thèse de Doctorat, Université de Cocody, Abidjan, Côte d'Ivoire, 283 p.

[5] Dibi, B. (2008) Cartographie des sites potentiels d'implantation des points d'eau dans le département d'Aboisso (Sud-Est de la Côte d'Ivoire): Apport du SIG et de l'analyse multicritère. Thèse unique de Doctorat, Université de Cocody, Abidjan, Côte d'Ivoire, 164 p.

[6] Eblin, S.G., Konan, K.S., Mangoua, M.J., Sandu, A.V., Barsan, N., Sandu, I. and Nedeff, V. (2019) Nitrate Pollution of Groundwater Based on GIS in the City of Daloa, West-Central Cote d'Ivoire. *Revista de Chimie* (*Bucharest*), **70**, 2579-2583. https://doi.org/10.37358/RC.19.7.7384

[7] Dibi, B., Kouassi, K.L., Kouamé, K.I., Konan, K.S., Soumahoro, M., Konan-Waidhet, A.B. and Gnakri, D. (2013) Assessment of the Vulnerability to Aquifer Pollution of Altered Formations Using DRASTIC and SYNTACS Methods: Case of the City of M'bahiakro, Central of Côte d'Ivoire. *International Journal of Innovation and Applied Studies*, **2**, 464-476.

[8] Mangoua, M.J., Konan, K.S., Kouamé, K.I., Zougrou, N.N., Kouassi, K.L., Savane, I. and Biemi, J. (2018) Assessment of Vulnerability to Groundwater Pollution in the Department of Tiassalé (South of Côte d'Ivoire). *EWASH & TI Journal*, **2**, 46-54.

[9] INS (2014) Institut National de la Statistiques. Abidjan, Côte d'Ivoire, 22 p.

[10] Yao, A.B. (2015) Evaluation des potentialités en eau du bassin versant de la lobo en

vue d'une gestion rationnelle (Centre-Ouest de la côte d'ivoire). Thèse Unique de Doctorat, Université Nangui Abrogoua, Abidjan, Côte d'Ivoire, 193 p.

[11] Tagini, B. (1971) Esquisse structurale de la Côte d'Ivoire. Essai de géotectonique régionale. Thèse de Doctorat, Université de Lausanne, Suisse, 302 p.

[12] Pothin, K. (1988) Pétrographie et géochimie des formations précambriennes de la région d'Odienné (Nord-Ouest de la Côte d'Ivoire). Thèse de Doctorat d'Etat Ès-Sciences Naturelles, Université de Cocody, Abidjan, 180 p.

[13] Dibi, B., Plagnes, V., Konan-Waidhet, A.B. and Savané, I. (2015) Définition d'une méthodologie de dimensionnement des zones de protection des ouvrages de captages d'eaux souterraines en zone de socle. Cas de la zone test du bassin versant d'Ehania (Sudest de la Côte d'Ivoire). Vingtièmes journées techniques du Comité Français d'Hydrogéologie de l'Association Internationale des Hydrogéologues. Aquifères de socle: Le point sur les concepts et les applications opérationnelles, La Roche-sur-Yon, 16 p.

[14] Petelet-Giraud, E., Dörfliger, N. and Crochet, P. (2000) RISKE: Méthode d'évaluation multicritère de la vulnérabilité des aquifères karstiques. Application aux systèmes des Fontanilles et cent-fonts (Hérault, sud de la France). *Hydrogéologie*, **4**, 71-88.

[15] Plagnes, V., Théry, S., Fontaine, L., Bakalowicz, M. and Doerfliger, N. (2005) Karst Vulnerability Mapping: Improvement of the RISKE Method. *KARST* 2005, *International Conference and Field Seminar*, *Water Resources and Environmental Problems in Karst*, Belgrade-Kotor, Serbia, 14-19 September 2005.

[16] Durand, L. (2012) Cartographie de la Vulnérabilité du Système Karstique des Eaux Belles (Haute-Savoie) et étude de son Fonctionnement. Master 2 Sciences de l'univers, Environnement, Ecologie. Université Pierre et Marie Curie, École des Mines de Paris & École Nationale du Génie Rural des Eaux et des Forêts. Parcours Hydrologie Hydrogéologie, 45 p.

[17] Kavouri, D. (2008) Evaluation cartographique de la vulnérabilité des eaux souterraines de la partie nord du Causse de Gramat (Lot). Rapport Université Pierre et Marie Curie-Paris 6/PnrCQ, disponible prochainement sur le site de l'AEAG.

[18] Mangoua, O.M.J., Kouassi, K.A., Kouassi, W.F., Douagui, G.A., Savane, I. and Biemi, J. (2020) Assessment of Vulnerability to Groundwater Pollution in Department of Odienné (North-West Côte d'Ivoire). *African Journal of Science*, *Technology*, *Innovation and Development*, **12**, 297-303.
https://doi.org/10.1080/20421338.2020.1742481

[19] Dörfliger, N. and Plagnes, V. (2010) Cartographie de la vulnérabilité de l'aquifère karstique guide méthodologique de la méthode PaPRIKa. Rapport BRGM, Orleans, France, 100 p.

[20] Saaty, T.L. (1977) A Scaling Method for Priorities in Hierarchical Structures. *Journal of Mathematical Psychology*, **15**, 234-281.
https://doi.org/10.1016/0022-2496(77)90033-5

[21] Doumouya, I., Dibi, B., Kouamé, K.I., Saley, B., Jourda, J.P., Savane, I. and Biemi, J. (2012) Modelling of Favourable Zones for the Establishment of Water Points by Geographical Information System (GIS) and Multicriteria Analysis (MCA) in the Aboisso Area (South-East of Côte d'Ivoire). *Environmental Earth Science*, **67**, 1763-1780. https://doi.org/10.1007/s12665-012-1622-2

[22] Office fédéral de l'environnement, des forêts et du paysage (OFEFP), Office fédéral des eaux et de la géologie (OFEG) (2003) Délimitation des zones de protection des eaux souterraines en milieu fissuré. Guide Pratique. Berne, 2003.
https://www.bafu.admin.ch/dam/bafu/fr/dokumente/wasser/uv-umwelt-vollzug/aus

schei-
dung_vongrundwasserschutzzonenbeikluft-grundwasserleiter.pdf.download.pdf/delimitation_deszonesdeprotectiondeseauxsouterrainesenmilieufiss.pdf

[23] Murat, V., Martel, R., Michaud, Y. and Therrien, R. (2000) Etude comparative des méthodes d'évaluation de la vulnérabilité des aquifères à la pollution: Application aux aquifères granulaires du Piémont Laurentien, Québec. AIH-CNC et SCG, 411-418.

[24] Kouadio, A.N.B. (2019) Évaluation du risque sanitaire lié à la consommation des eaux de puits traditionnels par les ménages à faibles revenus en milieu urbain: Cas de la ville d'Agboville (Côte d'Ivoire). Thèse Unique de Doctorat, Université Nangui Abrogoua, Abidjan, Côte d'Ivoire, 188 p.

[25] Mangin, A. (1975) Contribution à l'étude hydrodynamique des aquifères karstiques [Contributions to the Hydrodynamics of Karst Aquifers]. Thèse, Université Dijon (France), Dijon, 124 p.

[26] Prasad, R.K., Mondal, N.C., Pallavi, B., Nandakumar, M.V. and Singh, V.S. (2008) Deciphering Potential Groundwater Zone in Hard Rock through the Application of GIS. *Environmental Geology*, **55**, 467-475.
https://doi.org/10.1007/s00254-007-0992-3

[27] Mohamed, R.M. (2001) Evaluation et cartographie de la vulnérabilité à la pollution de l'aquifère alluvionnaire de la plaine d'El Madher, Nord-Est algérien, selon la méthode DRASTIC. *Sciences et Changements Planétaires/Sécheresse*, **12**, 95-101.

[28] Mohamed, S., Rachid, M. and Moumtaz, R. (2003) Utilisation des SIG pour la caractérisation de la vulnérabilité et de la sensibilité à la pollution des nappes d'eau souterraine. Application à la nappe du Haouz de Marrakech, Maroc. *Management of Water Resources*, **2**, 1-15.

[29] Panagopoulos, G.P., Antonakos, A.K. and Lambrakis, N.J. (2006) Optimization of the DRASTIC Method for Groundwater Vulnerability Assessment via the Use of Simple Statistical Methods and GIS. *Hydrogeology Journal*, **14**, 894-911.
https://doi.org/10.1007/s10040-005-0008-x

[30] Aké, G.E., Kouadio, H.B., Dongo, K., Dibi, B., Kouamé, F.K. and Biémi, J. (2010) Application des méthodes DRASTIC et SI pour l'étude de la vulnérabilité à la pollution par les nitrates (N03-) de la nappe de Bonoua (Sud-Est de la Côte d'Ivoire). *International Journal of Biological and Chemical Sciences*, **4**, 1675-1692.
https://doi.org/10.4314/ijbcs.v4i5.65557

[31] Eblin, S.G. (2014) Dégradation des écosystèmes environnementaux dans la région d'Adiaké (Sud-Est côtier de la côte d'ivoire) et risque de pollution des eaux: Apport d'un sig. Thèse d'Université Félix Houphouët Boigny de Cocody (Côte d'Ivoire), 248 p.

[32] Hamza, M.H., Added, A., Frances, A. and Rodriguez, R. (2007) Validité de l'application des méthodes de vulnérabilité DRASTIC, SINTACS et SI à l'étude de la pollution par les nitrates dans la nappe phréatique de Metline-Ras Jebel-Raf Raf (Nord-Est tunisien). *Comptes rendus Géosciences*, **339**, 493-505.
https://doi.org/10.1016/j.crte.2007.05.003

[33] Deh, K.S., Kouamé, K.J., Saley, M.B., Tanoh, K.J.J., Anani, K.H., Signo, J., Jourda, J.P. and Biémi, J. (2012) Evaluation de la vulnérabilité spécifique aux nitrates (NO_3) des eaux souterraines du District d'Abidjan (Sud de la Côte d'Ivoire). *International Journal of Biological and Chemical Sciences*, **6**, 1390-1408.
https://doi.org/10.4314/ijbcs.v6i3.40